Telomerase reverse transcriptase protects ATM-deficient hematopoietic stem cells from ROS-induced apoptosis through a telomere-independent mechanism

Eriko Nitta,[1,2] Masayuki Yamashita,[1] Kentaro Hosokawa,[1] MingJi Xian,[1] Keiyo Takubo,[1] Fumio Arai,[1] Shinichiro Nakada,[3] and Toshio Suda[1]

[1]Department of Cell Differentiation, The Sakaguchi Laboratory of Developmental Biology, Keio University School of Medicine, Tokyo, Japan; [2]Japan Society for the Promotion of Science, Tokyo, Japan; and [3]Center of Integrated Medical Research, Keio University School of Medicine, Tokyo, Japan

Telomerase reverse transcriptase (TERT) contributes to the prevention of aging by a largely unknown mechanism that is unrelated to telomere lengthening. The current study used ataxia-telangiectasia mutated (ATM) and TERT doubly deficient mice to evaluate the contributions of 2 aging-regulating molecules, TERT and ATM, to the aging process. ATM and TERT doubly deficient mice demonstrated increased progression of aging and had shorter lifespans than ATM-null mice, while TERT alone was insufficient to affect lifespan. ATM-TERT doubly null mice show in vivo senescence, especially in hematopoietic tissues, that was dependent on $p16^{INK4a}$ and $p19^{ARF}$, but not on p21. As their HSCs show decreased stem cell activities, accelerated aging seen in these mice has been attributed to impaired stem cell function. TERT-deficient HSCs are characterized by reactive oxygen species (ROS) fragility, which has been suggested to cause stem cell impairment during aging, and apoptotic HSCs are markedly increased in these mice. p38MAPK activation was indicated to be partially involved in ROS-induced apoptosis in TERT-null HSCs, and BCL-2 is suggested to provide a part of the protective mechanisms of HSCs by TERT. The current study demonstrates that TERT mitigates aging by protecting HSCs under stressful conditions through telomere length-independent mechanisms. (*Blood*. 2011;117(16):4169-4180)

Introduction

Aging is accompanied by a number of pathophysiologic changes in the hematopoietic system. The etiology of these changes suggests that loss of homeostatic control and regenerative potential is driven by diminution of stem cell reserves.[1] Although growing evidence indicates that the maintenance of telomere length is important in aging, these observations raise the question that telomerase might have major functions that are unrelated to telomere lengthening.[2-4] Also implying a nontelomere aging-related mechanism, mouse cells have a massive telomere reserve compared with human cells.[5] Although previous reports have shown that telomerase reverse transcriptase (TERT) is essential for the long-term reconstitution ability of HSCs, they have failed to demonstrate that HSC activities are fully dependent on the telomere-elongation function of TERT.[6,7] On the other hand, more recent experiments have strongly suggested that TERT may have a telomere-independent role in stem cell maintenance. The ectopic expression of TERT in the hair follicle stem cells of mouse epidermis activates stem cell capacities in the absence of detectable telomere elongation.[8-10] Moreover, activation of TERT in cancer-resistant mice extends lifespan.[11,12] Taken together, these previous studies suggest that TERT plays a critical telomere-independent role in extending lifespan by promoting stem cell activity, at least in mice.

Meanwhile, ataxia-telangiectasia mutated (ATM) is a causative gene for hereditary progeria syndrome, also known as ataxia-telangiectasia (AT). AT is characterized by premature aging, immunodeficiency, progressive cerebellar ataxia, oculocutaneous telangiectasia, and a high incidence of lymphoma. It has been shown that impaired ATM function leads to defects in the control of reactive oxygen species (ROS). It has been reported that oxidative stress levels are increased in tissues from AT patients, although the mechanism by which ATM regulates ROS levels is unclear.[13,14] We have previously reported a critical role for ATM in stem cell self-renewal because of its effects on ROS regulation during hematopoiesis. Furthermore, treatment with the antioxidative agent *N*-acetyl-L-cysteine (NAC) prevents the BM failure observed in ATM-deficient mice, suggesting that stem cell depletion or dysfunction might contribute to the premature aging that characterizes AT.[15,16]

While ATM has well-understood, critical roles in aging that involve protecting HSCs from ROS elevation and DNA damage accumulation,[17,18] the precise role of TERT in maintaining stem cell activity is unclear. TERT activity is restricted to primitive stem cells and progenitor cells, and we therefore hypothesized that TERT has important functions that serve to protect stem cells and progenitor cells from various stresses. As aging is associated with a rise in the levels of various extra- or intracellular stresses, including ROS and DNA damage, the function of TERT in aging is suggested to involve the regulation of cellular stress mitigation by ATM. Therefore, to investigate the telomere length-independent function of TERT in aging and stem cell maintenance, we evaluated TERT-deficient HSCs in an ATM-null background. We demonstrated that TERT is an important regulator that exerts its influence on the aging process by maintaining stem cells in an ATM-null background, namely under various cellular stress conditions, through telomere length-independent mechanisms.

Submitted August 2, 2010; accepted January 17, 2011. Prepublished online as *Blood* First Edition paper, February 4, 2011; DOI 10.1182/blood-2010-08-297390.

The online version of this article contains a data supplement.

The publication costs of this article were defrayed in part by page charge payment. Therefore, and solely to indicate this fact, this article is hereby marked "advertisement" in accordance with 18 USC section 1734.

Methods

Mice

ATM mutant heterozygous mice[19] (a gift from P. J. McKinnon; St Jude Children's Research Hospital, Memphis, TN) and TERT mutant heterozygous mice[20] (a gift from Fuyuki Ishikawa; Kyoto University, Kyoto, Japan) were mated to obtain $ATM^{-/-}TERT^{-/-}$ mice. Littermates or age-matched control mice were used as controls in all experiments. C57BL/6 mice congenic for the CD45 locus (B6-Ly5.1) were purchased from Sankyo-Lab Service. Animal care in our laboratory was in accordance with the guidelines for animal and recombinant DNA experiments of Keio University. NAC was administrated orally (40mM in drinking water) for 4 weeks.

SA-β-galactosidase assay

For the SA-β-galactosidase assay, cryosections (10 μm) of OCT frozen tissue were used. SA-β-galactosidase activity was determined using a senescence detection kit (Cell Signaling Technology) according to the manufacturer's instructions. Senescent cells were identified as blue-stained cells under an IX70 inverted microscope (Olympus). Images are obtained with DP70 camera and DP Controller software Version 3.1 (Olympus).

Immunohistochemistry on paraffin sections

Organs were fixed in 4% paraformaldehyde (PFA) overnight and embedded in paraffin. For antigen retrieval, 4 μm-thick sections of the prepared organs were deparaffinized and heated by microwave in tris buffer (pH 10.0) with 0.1% Tween for 5 minutes. Sections were stained with anti-p16 (NeoMarkers 1:50), anti-p19 (Abcam 1:100), anti-p21 (Abcam 1:100), anti–phospho-p53 (Abcam 1:25), or anti-γH2AX (Millipore 1:100) antibody. Sections were examined under an IX70 light microscope (Olympus), and images were captured with an Olympus digital DP70 camera using DP Controller software Version 3.1.

Flow cytometry and cell sorting

Monoclonal antibodies (mAbs) recognizing the following markers were used for flow cytometric analysis and cell sorting (FACS Calibur, FACS Vantage or FACS Aria; BD Bioscience): c-Kit (2B8), Sca-1 (D7), CD4 (L3T4), CD8 (53-6.7), B220 (RA3-6B2), TER-119 (Ly-76), Gr-1 (RB6-8C5), CD34 (RAM34), CD45.1 (A20), CD45.2(104) Mac-1 (M1/70), CD3 (500A2), and CD19 (1D3). All mAbs were purchased from BD Biosciences. A mixture of mAbs recognizing CD4, CD8, B220, TER-119, Mac-1, or Gr-1 was used to identify lineage-positive cells.

Immunocytochemistry

Immunocytochemistry was performed as previously described.[21] Briefly, sorted cells were put onto a glass slide, fixed with 4% PFA, and stained with anti-H3K9Me (Upstate Biotechnology; 1:200), anti-HP1γ (Abcam; 1:200), anti-γH2AX (Millipore; 1:200), anti-TRF1 (Santa Cruz Biotechnology; 1:50), anti-53BP1 (Novus Biologicals; 1:200), or anti–phospho-p38 (CST, 1:500) antibody. Nuclei were identified by staining with DAPI (Invitrogen) or TOTO3 (Invitrogen). Subcellular localizations were determined using an FV1000 confocal laser-scanning microscope and FV10-ASW software Version 2.0 (Olympus).

Cell-Cycle Analyses

To analyze cell-cycle status, freshly isolated BM-MNCs were first stained using antibodies against cell-surface markers, and then fixed and stained using anti-Ki67 antibody (BD Biosciences) and Hoechst 33342, as previously described.[22]

BrdU incorporation analysis was performed using a FITC BrdU Flow Kit (Pharmingen) after intraperitoneal injection of 100 mg of BrdU (Sigma-Aldrich) per 1 kg of mouse weight twice every 12 hours. At 12 hours after injection, LSKs were collected from BM, fixed, and stained with Hoechst 33342 and anti-BrdU antibody (BD Biosciences), as previously described.[22]

BM competitive reconstitution assay

Sorted 2×10^3 lineage-negative, Sca-1^+, and c-Kit^+ cells (LSKs) from donor mice were transplanted into lethally irradiated B6-Ly5.1 congenic mice with 2×10^5 BM-MNCs from B6-Ly5.1 competitor mice. The reconstitution of donor-derived cells (Ly5.2) was monitored by staining peripheral blood (PB) cells or BM-MNCs with mAbs against CD45.2 and CD45.1. For the serial transplantation analysis, 2×10^3 donor-derived LSKs were harvested from recipient mice at 16 weeks after the first bone marrow transplantation (BMT) and transplanted into a second set of lethally irradiated recipient mice (second BMT).

Quantification of telomere length and telomere FISH

Telomere length was quantified by flow cytometry using flow FISH with a Telomere PNA Kit/FITC for flow cytometry (Dako Cytomation), according to the manufacturer's instructions. Briefly, freshly isolated cells were divided into 2 aliquots, denatured in hybridization solution with or without telomere-PNA probes, and hybridized overnight. After washing and DNA staining, labeled or nonlabeled (as control) samples were analyzed on a flow cytometer.

For telomere FISH, freshly isolated BM cells were incubated in nocodazole for 90 minutes and then metaphase spread slides were prepared with these cells. Telomere FISH was performed with a Telomere PNA Kit/Cy3 (Dako Cytomation) according to the manufacturer's instructions.

Intracellular ROS assay

To analyze intracellular ROS levels, cells were incubated with 300nM CM-H_2-DCFDA (Invitrogen) at 37°C for 15 minutes, followed by analysis of fluorescence by flow cytometry.

Apoptosis analysis

To assay apoptosis, cells stained for cell-surface markers were further incubated for 15 minutes with annexin V and propidium iodide (PI) as per the manufacturer's protocol using the Annexin V–FITC Apoptosis Detection Kit (Pharmingen).

For the analysis of ROS-induced apoptosis, freshly isolated LSKs were cultured in SF-O3 medium with 100 ng/mL murine stem cell factor and 100 ng/mL human thrombopoietin, adding buthionine sulfoximine (BSO; 100μM) and/or NAC (100-1000μM) for 12 hours as previously described.[16] For the experiments involving MAPK inhibitors, we incubated the BSO-treated LSKs with SB203580 (p38MAPK inhibitor, 10-100μM) or SP600125 (JNK inhibitor, 1-10μM).

Statistical analysis

P values were calculated using the unpaired Student *t* test for all data except survival data. The survival rates of mice of each genotype were analyzed using a log-rank nonparametric test.

Results

ATM and TERT double deficiency impairs cellular and whole-organism viability

First, we examined the impact of ATM and TERT double deficiency at the whole-organism level in $ATM^{-/-}TERT^{-/-}$ mice (Figure 1A). Consistent with a previous report,[20,23] WT and $TERT^{-/-}$ cohorts both survived for 2 years, indicating that TERT deficiency by itself does not influence survival. One-third of the $ATM^{-/-}$ mice succumbed to thymic lymphoma, as we have previously reported[15]; another third developed solid tumors; and the rest died from unknown causes. The median latency was 43 weeks. In contrast, the absence of TERT led to suppression of lymphoma development in $ATM^{-/-}$ mice. Despite lymphoma resistance, however, the median lifespan of the $ATM^{-/-}TERT^{-/-}$ mice was significantly

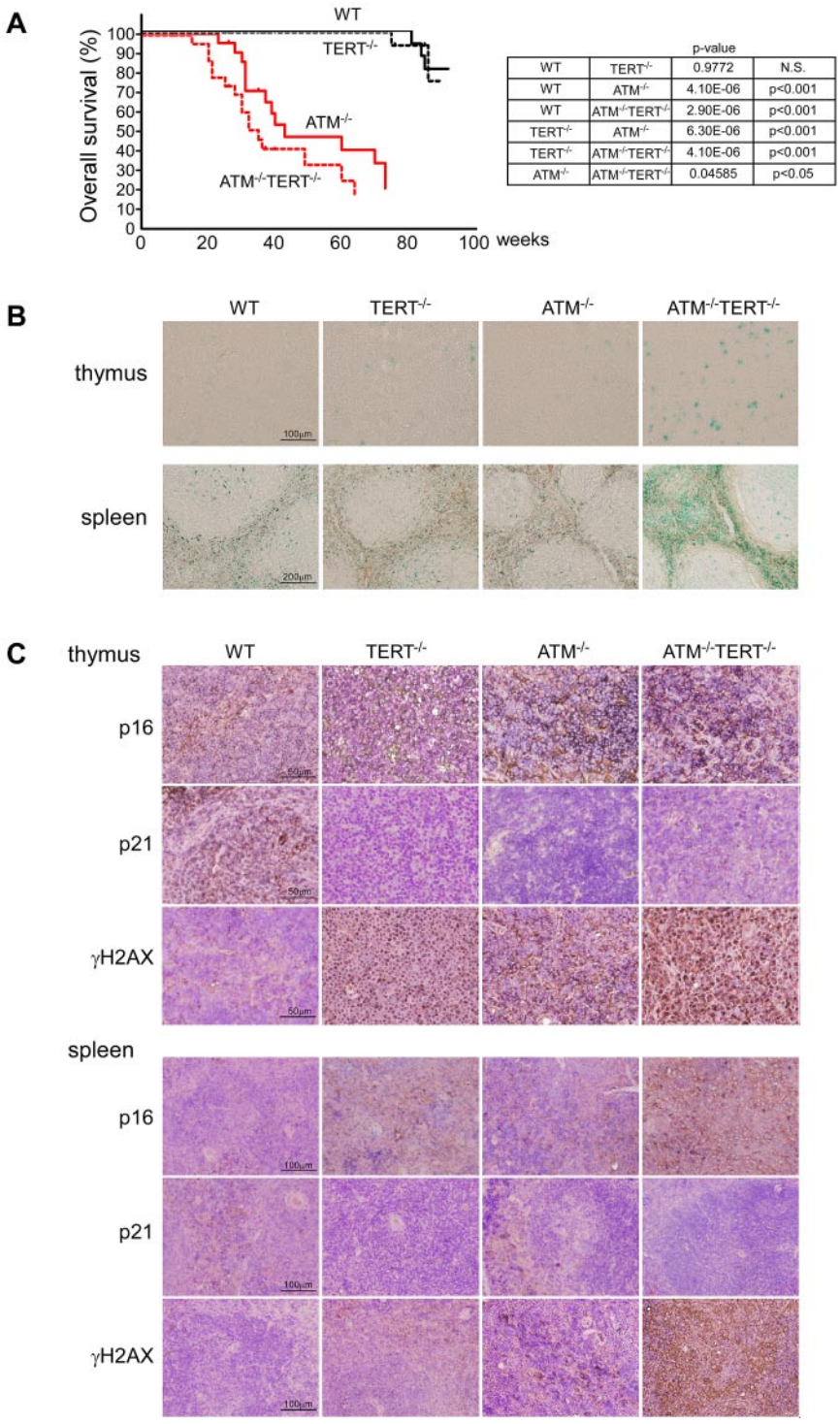

Figure 1. Cellular and whole-organism viability is impaired in ATM and TERT doubly null mice. (A) Survival curves for mice of the indicated genotypes (left). $ATM^{-/-}TERT^{-/-}$ mice had shorter longevity than $ATM^{-/-}$ mice. Data shown are survival rates expressed as a percentage. Results were analyzed with a log-rank nonparametric test (right). (B) SA-β-gal staining of frozen sections of thymus and spleen taken from mice of the indicated genotypes (12 weeks of age). Tissues taken from $ATM^{-/-}TERT^{-/-}$ mice demonstrated increased SA β-gal staining, compared with other littermates. (C) Immunohistochemical analysis against p16, p21, and γH2AX in thymus and spleen from mice of the indicated genotypes (36 weeks of age). While p16 is increased in sections from $TERT^{-/-}$, $ATM^{-/-}$, and $ATM^{-/-}TERT^{-/-}$ mice, p21 is decreased in these sections. γH2AX is also increased, especially in the $ATM^{-/-}$ and $ATM^{-/-}TERT^{-/-}$ thymus and spleen.

shorter (35 weeks) than that of the $ATM^{-/-}$ controls. There was no immediately obvious reason for this. Specifically, with only 3 exceptions (leukemia in 1 case and abdominal tumor in 2 others) among the 24 observed mice, there was no discernible prodrome (no accelerated weight loss, cachexia, reduced food and fluid intake, or change in activity level). Extensive analysis at autopsy failed to reveal a definitive cause of death in almost all (21 of 24) of the $ATM^{-/-}TERT^{-/-}$ mice.

To elucidate the cause of death for $ATM^{-/-}TERT^{-/-}$ mice, we evaluated senescence-associated endogenous β-galactosidase (SA β-gal) activity in 5 organs in young mice and aged mice (Figure 1B, and supplemental Figure 1A-B, available on the *Blood* Web site; see the Supplemental Materials link at the top of the online article). Thymus, spleen, kidney, liver, and intestine tissue sections from young and aged WT, $TERT^{-/-}$, $ATM^{-/-}$, and $ATM^{-/-}TERT^{-/-}$ littermate mice (12 weeks of age and 43 weeks of age) were stained with SA β-gal. Young $ATM^{-/-}TERT^{-/-}$ animals demonstrated marked increases in SA β-gal staining in thymus, spleen, and intestine, equivalent to the levels in aged mice, but there were no differences in SA β-gal staining in kidney and liver sections among the 4 groups. In the intestine, especially within intestinal crypts, cells showed high SA β-gal activity. On the other hand, aged

animals demonstrated comparable SA β-gal staining among the 4 groups in all 5 of these organs.

To further clarify the mechanisms of aging, we assessed several senescence marker proteins in these organs in aged mice by immunohistochemical analysis. Paraffin sections of 5 organs from aged WT, TERT$^{-/-}$, ATM$^{-/-}$, and ATM$^{-/-}$TERT$^{-/-}$ mice (36 weeks of age) were stained using anti-p16, p19, p21, phospho-p53, and γH2AX antibodies. Expression of p16 and p19 demonstrated increases in TERT$^{-/-}$, ATM$^{-/-}$, and ATM$^{-/-}$TERT$^{-/-}$ mice in thymus and spleen (Figure 1C and data not shown). In contrast to these proteins, p21 was decreased in these mutant mice. The levels of phospho-p53 were comparable among all groups. γH2AX increased in these mutant mice, especially in ATM$^{-/-}$ and ATM$^{-/-}$TERT$^{-/-}$ mice. In contrast, all of these senescence markers were expressed equally among the 4 groups in kidney, liver, and intestine (supplemental Figure 1C). In intestine, these proteins were weakly positive in villus epithelial cells but not in cells within intestinal crypts. This indicates that SA β-gal activity in cells within intestinal crypts may not reflect senescent status. There was also no histologic abnormality in these 5 organs of young mice by H&E stain (supplemental Figure 1D).

These results suggested that TERT or ATM deficiency contributes to in vivo senescence in the hematopoietic system especially in young mice, and also generally influences aging at the whole-organism level.

Aging phenotypes in the hematopoietic systems of ATM$^{-/-}$TERT$^{-/-}$ mice

Aging is accompanied by a number of pathophysiologic changes in the hematopoietic system. Histologic analysis of femurs showed progressed hypoplastic fatty marrow in aged TERT$^{-/-}$ mice and this condition was even more progressed in aged ATM$^{-/-}$TERT$^{-/-}$ mice. It was not seen in young mice (Figure 2A). SA-β-gal staining of BM is mildly enhanced in aged TERT$^{-/-}$, ATM$^{-/-}$, and ATM$^{-/-}$TERT$^{-/-}$ mice in cells near the proximal metaphysis (supplemental Figure 2A).

Extensive evidence indicates that HSC numbers increase substantially with advancing age in common strains of laboratory mice.[24-27] As is typical in aged individuals, in the BM of aged ATM$^{-/-}$TERT$^{-/-}$ mice, there was an apparent increase in the population of LSKs. This was more obvious in CD34$^-$ LSKs. We also demonstrated that the population of CD150$^+$, CD48$^-$ and CD41$^-$ LSKs was increased in the BM of ATM$^{-/-}$TERT$^{-/-}$ mice. Although this population increase was already seen in young ATM$^{-/-}$TERT$^{-/-}$ HSCs, the increase was greater in the HSCs of aged mice (Figure 2B and supplemental Figure 2B). The HSC population increase in these animals was accompanied by a marked myeloid lineage bias. Namely, large increases in the populations of myeloid lineage cells harboring Gr-1 and Mac-1 were seen in the BM of ATM$^{-/-}$TERT$^{-/-}$ mice. In addition, decreases in lymphoid lineages, including B and T cells, were seen, especially in aged ATM$^{-/-}$ and TERT$^{-/-}$ BM samples. These changes were even more obvious in ATM$^{-/-}$TERT$^{-/-}$ mice. Regarding T cells, CD4$^+$ helper T cells and CD8$^+$ cytotoxic T cells were both decreased in ATM$^{-/-}$TERT$^{-/-}$ mice.[28] This "myeloid shift" was also greater in aged BM (Figure 2C and supplemental Figure 2C). The myeloid lineage bias seen in aged HSCs may result from clonal expansion of stem cells with a myeloid bias during aging.[29-31] We next addressed lineage differentiation in thymus and spleen in aged mice, and this analysis revealed no apparent difference except for a decrease in CD3 expression in ATM$^{-/-}$ and ATM$^{-/-}$TERT$^{-/-}$ mice (supplemental Figure 2D).

To evaluate the cytologic status of HSCs in these mice, we further performed immunocytochemical analyses. DAPI staining elucidated that CD34-negative LSKs isolated from TERT$^{-/-}$ or ATM$^{-/-}$TERT$^{-/-}$ mice formed a characteristic chromatin condensation. These cells were stained with anti–methylated histone H3 at Lys9 (H3K9me) and anti–heterochromatin protein 1γ (HP1γ) antibodies, because H3K9me and HP1γ are proteins typically detected in heterochromatin. The DAPI-stained chromatin foci merged with both the H3K9me and HP1γ loci, suggesting that these foci represent heterochromatin (Figure 3A). It has been previously reported that senescent cells show characteristic heterochromatin foci called senescence-associated heterochromatic foci (SAHFs).[32,33] H3K9me is reported to be enriched at proliferation-promoting gene promoters, specifically in senescent cells showing SAHFs. This results in decreased expression of some of these genes, especially the E2F1 target gene.[32] We therefore measured the expression of the E2F1 target genes, cyclin A2 and proliferating cell nuclear antigen (PCNA). Transcription of cyclin A2 was suppressed in aged ATM$^{-/-}$TERT$^{-/-}$ HSCs and PCNA was suppressed in aged TERT$^{-/-}$ and ATM$^{-/-}$TERT$^{-/-}$ HSCs, which was about the same degree in young mouse HSCs of all genotypes (Figure 3B). SAHFs have not been described in vivo and it is not clear whether the chromatin foci we observed in TERT$^{-/-}$ and ATM$^{-/-}$TERT$^{-/-}$ HSCs are defined as SAHFs. However, the observations do seem to be consistent with a state of senescence. Hence, we next evaluated the cell-cycle status of LSKs in native LSKs in these mice. The population of Ki67-negative (cell cycle–arrested) TERT$^{-/-}$ or ATM$^{-/-}$TERT$^{-/-}$ LSKs was increased relative to that of wild-type controls, whereas the population of ATM$^{-/-}$ arrested LSKs was significantly decreased (Figure 3C). A BrdU short-labeling assay also revealed that BrdU-negative LSKs were relatively increased in TERT$^{-/-}$ or ATM$^{-/-}$TERT$^{-/-}$ mice. Meanwhile, BrdU-low/positive cells in TERT$^{-/-}$ or ATM$^{-/-}$TERT$^{-/-}$ mice decreased compared with wild-type controls, whereas cycling ATM$^{-/-}$ LSKs significantly increased (Figure 3D). These findings indicate that the cell cycle in TERT$^{-/-}$ and ATM$^{-/-}$TERT$^{-/-}$ HSCs is likely to be in a state of cell-cycle arrest and is likely to be regulated in a TERT-dependent manner that is independent of coordination between ATM and TERT. Our findings comprise the first reports that show that cell cycle in aged HSCs is arrested, because the cell-cycle status in HSCs of such exceedingly aged mice has not been observed. Hence, further studies about aging status of HSCs will be needed. To clarify whether the inactivation of the cell cycle in TERT$^{-/-}$ and ATM$^{-/-}$TERT$^{-/-}$ HSCs is related to aging in these cells, we measured the expression of p16^{INK4a}, p19^{ARF}, and p21 as senescent markers in LSKs in aged mice (37 weeks of age: Figure 3E). Transcription of p16^{INK4a} and p19^{ARF} was elevated in TERT$^{-/-}$ and ATM$^{-/-}$TERT$^{-/-}$ HSCs. Although we previously demonstrated that p16^{INK4a} and p19^{ARF} expression increased in 24-week-old ATM$^{-/-}$ HSCs,[15] we found that the transcription level of these proteins was comparable between WT HSCs and ATM$^{-/-}$ HSCs in 37-week-old mice in this study. This may have resulted from the intensive elevation of the levels of these proteins that accompanies stem cell aging especially in WT HSCs. On the other hand, the transcription of p21 was suppressed in TERT$^{-/-}$, ATM$^{-/-}$ and ATM$^{-/-}$TERT$^{-/-}$ HSCs. These results are consistent with the expression of these senescent proteins in thymus and spleen except for the increase in p16 and p19 proteins in ATM$^{-/-}$ mice (Figure 1C). Further, considering our observation in TERT$^{-/-}$ and ATM$^{-/-}$TERT$^{-/-}$ HSCs, the effects can be reasonably classified as cell-cycle inactivation accompanied by stem cell aging regulated by p16^{INK4a} and p19^{ARF}, and not by p21.

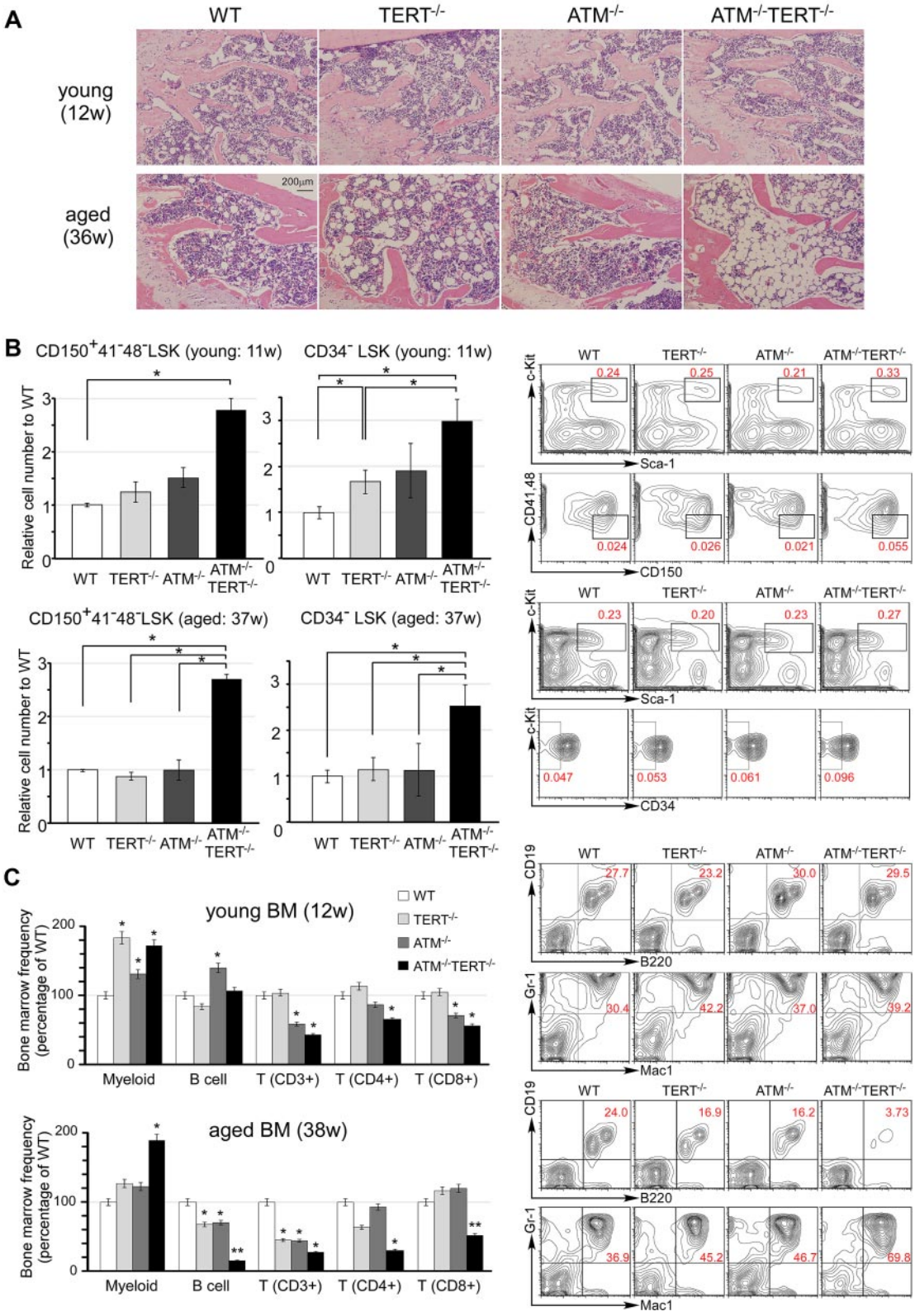

Figure 2. Pathophysiologic aging-related changes in the hematopoietic systems in ATM and TERT doubly null mice. (A) H&E staining of sections of decalcified femur, near the proximal metaphysis, from young mice (12 weeks of age: top) and aged mice (36 weeks of age: bottom). Progression of hypoplastic fatty marrow is apparent in aged $TERT^{-/-}$ mice, and significantly further progression in aged $ATM^{-/-}TERT^{-/-}$ mice, and is absent in young mice. (B) The numbers of $CD150^{+}$ $CD41^{-}$ $CD48^{-}$ LSKs and $CD34^{-}$ LSKs from $ATM^{-/-}TERT^{-/-}$ mice are increased compared with those of other genotypes. Relative numbers of the indicated fractions of BM cells from young (11 weeks of age: top) and aged (37 weeks of age: bottom) WT (white bar), $TERT^{-/-}$ (light-gray bar), $ATM^{-/-}$ (dark-gray bar), or $ATM^{-/-}TERT^{-/-}$ (black bar) mice (left). Representative FACS analyses of BM-MNCs in aged mice are also shown (right). Total cell numbers of indicated populations are compensated with body weight of each mouse and data shown are frequencies relative to those of WT, with each value representing the mean ± SD of 3 experiments (*$P < .05$). (C) Myeloid shift is observed in the BM of $TERT^{-/-}$, $ATM^{-/-}$, and $ATM^{-/-}TERT^{-/-}$ mice. The shift is most obvious in $ATM^{-/-}TERT^{-/-}$ mice and is also greater in aged mice (38 weeks of age: bottom) than in young mice (12 weeks of age: top). Frequency of each lineage (expressed as a percentage of WT: left) and representative FACS patterns of B-cell lineage and myeloid lineage (right) are shown for the indicated genotypes (*$P < .05$, **$P < .01$, n = 3).

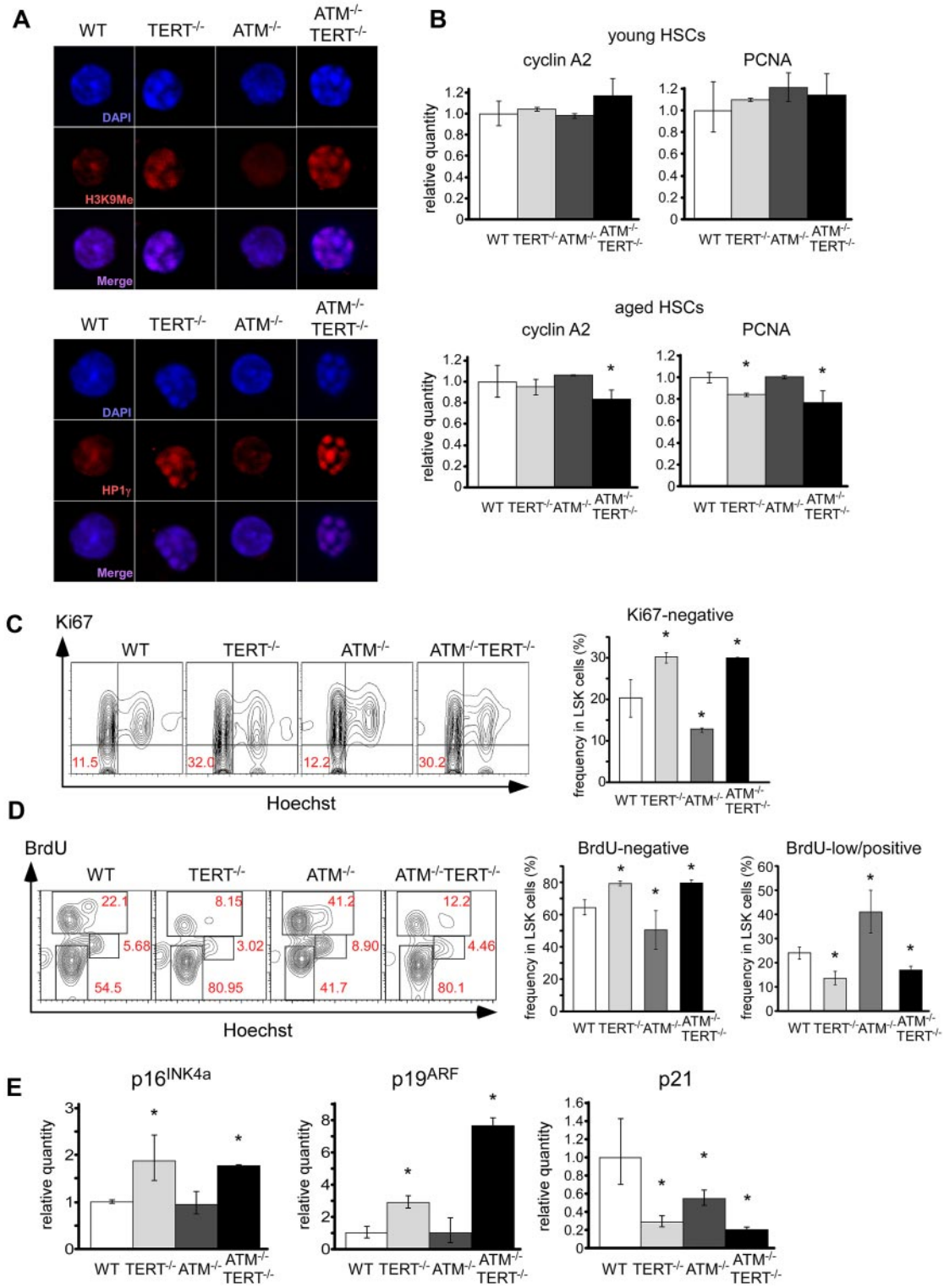

Figure 3. Cell-cycle arrest and increase of aging-related genes in TERT-deficient HSCs. (A) Foci of chromatin condensation in TERT$^{-/-}$ and ATM$^{-/-}$TERT$^{-/-}$ murine HSCs. CD34^{-}LSK cells from the indicated genotypes were stained with anti-H3K9Me Ab (top) or anti-HP1γ Ab (bottom). Nuclei were detected using DAPI staining (magnification ×1800). (B) qPCR analysis of proliferation-related genes in CD34^{-} LSKs from mice of the indicated genotypes. Reduced expression of cyclin A2 in aged TERT$^{-/-}$ murine HSCs and PCNA in aged TERT$^{-/-}$ and ATM$^{-/-}$TERT$^{-/-}$ murine HSCs (bottom), which is not seen in young HSCs (top). Data shown are the mean ratio (± SD) of mRNA to β-actin levels (*$P < .05$, n = 4). (C) Cell-cycle status of freshly isolated LSKs from mice of the indicated genotypes, assayed by Ki67 staining. TERT$^{-/-}$ and ATM$^{-/-}$TERT$^{-/-}$ LSKs showed increased Ki67-negative populations, whereas ATM$^{-/-}$ LSKs showed a reduced Ki67-negative population. Data shown are representative FACS patterns derived from 3 independent experiments (left); graphs show the mean (± SD) percentage of Ki67-negative cells (right; *$P < .05$). (D) Cell-cycle status of LSKs of each murine genotype, as evaluated by BrdU short-labeling assay. BrdU was administered for 24 hours to mark cells that entered S phase, and Hoechst was administered to detect DNA content. Representative FACS patterns derived from 3 independent experiments (left) and graphs showing the mean (± SD) percentage of BrdU-negative or BrdU-low/positive cells (right) are shown (*$P < .05$). TERT$^{-/-}$ and ATM$^{-/-}$TERT$^{-/-}$ LSKs showed relatively increased BrdU-negative populations and reduced BrdU-low/positive populations, whereas ATM$^{-/-}$ LSKs showed reduced BrdU-negative populations and increased BrdU-low/positive populations. (E) qPCR analysis of p16^{INK4a}, p19^{ARF}, and p21 in LSKs from aged mice of the indicated genotypes (37 weeks of age). Increased expression of p16^{INK4a} and p19^{ARF} in TERT$^{-/-}$ and ATM$^{-/-}$TERT$^{-/-}$ murine HSCs and reduced expression of p21 in these HSCs. Data shown are the mean ratio (± SD) of mRNA to β-actin levels (*$P < .05$, n = 3).

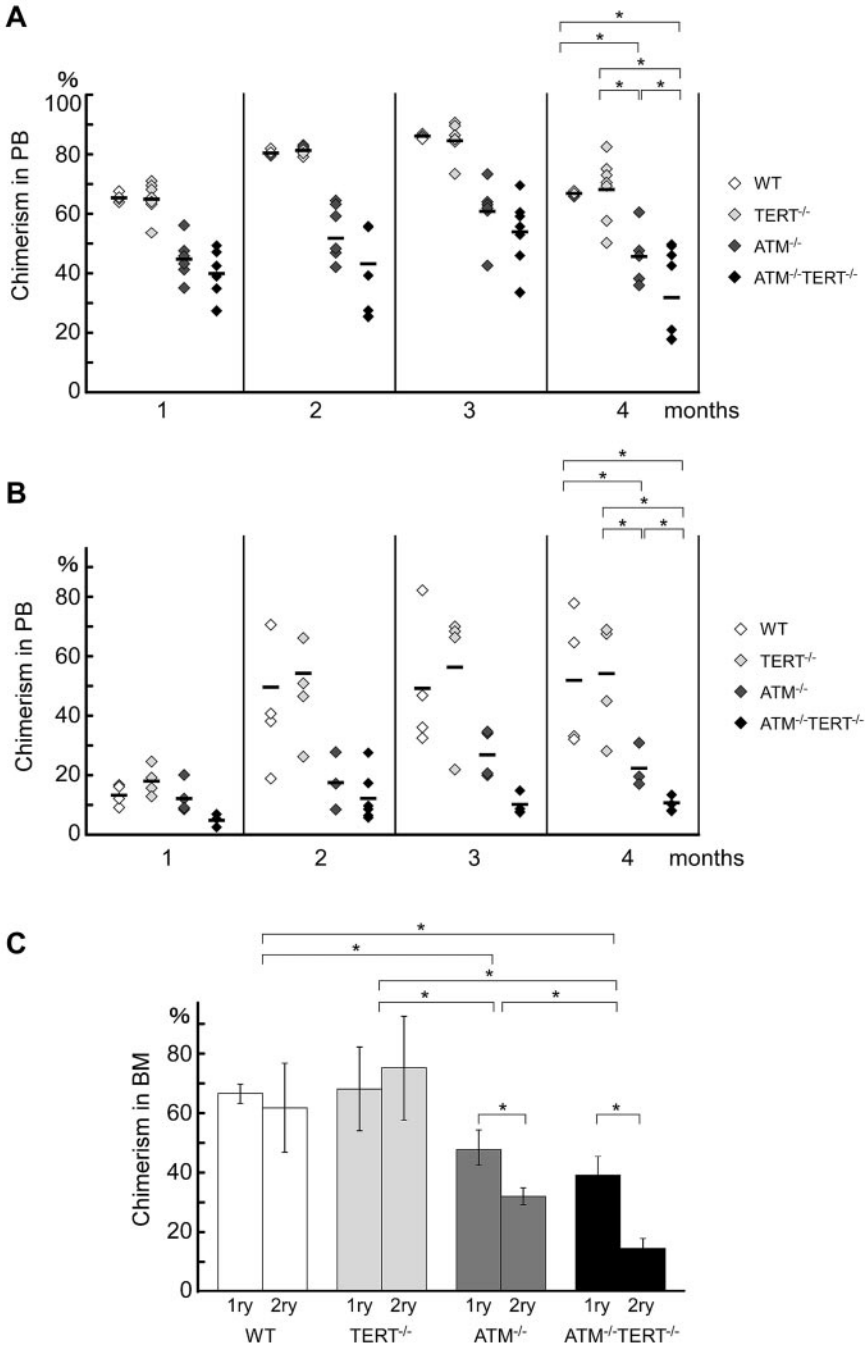

Figure 4. Hematopoietic stem cell capacities are abrogated in ATM and TERT doubly null mice. (A) Primary bone marrow transplantation: repopulation ability is impaired in $ATM^{-/-}TERT^{-/-}$ mice. Recipient mice were transplanted with 2×10^3 LSKs from mice of the indicated genotypes and 2×10^5 competitor BM-MNCs. Donor-derived chimerism of PB was analyzed monthly after transplantation. Data shown are the ratio (mean ratio: crossbar) of donor-derived cells in the competitive assay (*$P < .05$). (B) Second bone marrow transplantation: repopulation ability is again impaired in $ATM^{-/-}TERT^{-/-}$ LSKs. The repopulating capacity of donor cells of the indicated genotypes was determined as for primary transplantation. (C) Impaired long-term repopulation capacity in $ATM^{-/-}TERT^{-/-}$ LSKs during serial transplantation. Comparison of repopulation ability between primary and secondary transplantation for the indicated genotypes are represented. Data shown are the ratio (mean ratio: crossbar) of donor-derived cells in recipient BM (*$P < .05$).

HSCs exhibit abrogated self-renewal capacity in the absence of ATM and TERT

Models of aging often presuppose that the loss of homeostatic control and the regenerative potential of tissues are driven by the diminution of stem cell reserves. The proliferative and regenerative capacity of HSCs has also been suggested to diminish with age in an intrinsic and extrinsic manner. To assess whether these typical aging-related changes, which have been attributed to the attenuation of stem cell capacities, are seen in $ATM^{-/-}TERT^{-/-}$ mice, we performed a competitive reconstitution assay. In this assay, LSKs from WT, $TERT^{-/-}$, $ATM^{-/-}$, or $ATM^{-/-}TERT^{-/-}$ mice (Ly5.2) competed against BM-MNCs from a congenic (Ly5.1) mouse to reconstitute the hematopoietic compartment of an irradiated recipient mouse (Ly5.1). At 16 weeks after transplantation, flow cytometric analysis of PB and BM-MNCs of the transplant recipients revealed that $ATM^{-/-}TERT^{-/-}$ LSKs showed a severely impaired repopulating ability compared with $ATM^{-/-}$ LSKs, whereas wild-type and $TERT^{-/-}$ LSKs were equally capable of hematopoietic reconstitution (Figure 4A). A second competitive transplantation also showed that fewer hematopoietic cells were derived from $ATM^{-/-}TERT^{-/-}$ LSKs compared with $ATM^{-/-}$ LSKs at 16 weeks after the second BMT (Figure 4B). These data suggested that $ATM^{-/-}TERT^{-/-}$ HSCs had a diminished long-term repopulating capability and were eventually outcompeted by wild-type HSCs.

Nevertheless, the proportion of $ATM^{-/-}TERT^{-/-}$ LSK-derived cells at 16 weeks after the second BMT was reduced compared with that at 16 weeks after the first BMT (Figure 4C). This deficit is presumably caused by decreased repopulating capacity in the donor

cells on repeated BMT, whereas competitor BM cells continue to accumulate. These data confirm that TERT exerts a critical impact on the ability of HSCs to repopulate in an ATM-null background. Further, this observation suggests that many aging-related changes in the hematopoietic system are driven by HSC diminution in $ATM^{-/-}TERT^{-/-}$ mice.

Decreases in the HSC pool in ATM and TERT doubly deficient mice are independent of telomere length shortening or telomere dysfunction

Whereas TERT deficiency per se has little influence on in vivo aging or on normal hematopoietic stem cell function, there is little doubt that TERT plays a critical role in the activity of ATM-null HSCs. To investigate possible mechanisms for this, we first evaluated accumulated damage in these HSCs by measuring γH2AX foci in $CD34^{-}$LSKs in these mice. While γH2AX foci were only mildly increased in young $ATM^{-/-}$ and $ATM^{-/-}TERT^{-/-}$ mice, the numbers of γH2AX foci were increased in aged $ATM^{-/-}$ and $TERT^{-/-}$ LSKs, and were even further increased in $ATM^{-/-}TERT^{-/-}$ LSKs (Figure 5A). Although γH2AX foci generally represent DNA damage, controversy has recently arisen regarding the significance of γH2AX accumulation in HSCs.[34,35] However, as γH2AX is known to increase in senescent cells, γH2AX accumulation should represent aging status also in HSCs.[36,37]

Next, we measured the telomere length of WT, $ATM^{-/-}$, $TERT^{-/-}$ and $ATM^{-/-}TERT^{-/-}$ LSKs by flow FISH. No alteration in telomere length was seen following the loss of TERT, ATM, or the combination of ATM and TERT (Figure 5B).

Further, to evaluate whether accumulated damage in aged HSCs in these mutant mice arises from telomere dysfunction, we measured telomere free ends by telomere FISH (Figure 5C) and telomere dysfunction-induced foci (TIFs; Figure 5D). Telomere FISH using a metaphase spread revealed that telomere loss was not detected in the cells of mice of any of the genotypes. To detect more precise damages to the telomere, we stained LSKs isolated from BM with anti-TRF1 and anti-53BP1 antibodies, and then counted merged signals as TIFs.[38,39] No increase of TIFs were detected in $TERT^{-/-}$, $ATM^{-/-}$ and $ATM^{-/-}TERT^{-/-}$ LSKs than in WT LSKs. These results indicated that telomere dysfunctions are not also associated with the loss of TERT, ATM or the combination of TERT and ATM in HSCs.

Apoptosis is induced in ATM and TERT doubly null HSCs as a result of ROS fragility and is regulated by p38MAPK and BCL-2 family proteins

We previously reported that the reduced repopulating capacity of $ATM^{-/-}$ HSCs is accompanied by elevation of intracellular ROS.[16] Therefore, we next evaluated ROS levels in LSKs in these mice. We found that ROS levels in $ATM^{-/-}TERT^{-/-}$ LSKs were markedly higher than those in WT or $TERT^{-/-}$ LSKs, and were comparable to those in $ATM^{-/-}$ LSKs (Figure 6A).

Some evidence suggests that apoptosis may play a critical role in the regulation of HSCs,[40,41] although the precise nature of this role remains largely unknown. To address the mechanisms through which $ATM^{-/-}TERT^{-/-}$ HSCs impair stem cell capacity, we analyzed apoptosis in LSKs in these mice using annexin V and PI staining. Interestingly, $ATM^{-/-}TERT^{-/-}$ LSKs demonstrated pronounced increases in apoptosis compared with LSKs of the other genotypes (Figure 6B). Strikingly, this increase in apoptosis was detected only in $CD34^{-}$ or $CD150^{+}$ LSKs, representing HSCs, but not in $CD34^{+}$ or $CD150^{-}$ LSKs, representing progenitor cells.

Because ATM single deficiency did not contribute to an increase in apoptosis despite comparable ROS levels to those in $ATM^{-/-}TERT^{-/-}$ LSKs, we hypothesized that the TERT protein may play a critical role in the protection of $ATM^{-/-}$ HSCs from apoptosis induced by intracellular stresses. While antiapoptotic roles for TERT have been demonstrated in human cancer cell lines,[42,43] such roles in physiologic systems in vivo are not yet clear. To address this question, we evaluated the effect of ROS on HSCs in these mice. Treatment in vitro with BSO, an oxidant, for 12 hours significantly increased apoptosis in $TERT^{-/-}$, $ATM^{-/-}$, and $ATM^{-/-}TERT^{-/-}$ LSKs, in contrast to that BSO treatment did not induce apoptosis in WT LSKs. In addition to the apoptosis induced by BSO, culture in vitro without BSO did also lead to some apoptosis in $ATM^{-/-}TERT^{-/-}$ LSKs. The substantial apoptotic effect by BSO was rescued by adding NAC, an antioxidant, in a dose-dependent manner to these LSK cultures (Figure 6C). These data indicated that the TERT protein contributes to the survival of $ATM^{-/-}$ HSCs by acting against apoptosis induced by ROS. To replicate this rescue from the ROS-induced apoptotic effect by NAC in vivo, we decreased the ROS in cells of 8-week-old WT, $TERT^{-/-}$, $ATM^{-/-}$, and $ATM^{-/-}TERT^{-/-}$ mice by orally administering NAC for 4 weeks. We found that treatment of $ATM^{-/-}TERT^{-/-}$ mice with NAC rescued their HSCs from apoptosis (Figure 6D).

We next investigated the nature of the molecular mechanism underlying the action of TERT on ROS-induced apoptosis. To address this issue, we focused on 2 MAPKs, p38MAPK and JNK, as we have previously reported that the ROS-p38MAPK pathway is involved in stem cell dysfunction in $ATM^{-/-}$ HSCs.[16] We first determined the activation status of p38MAPK in LSKs in mice with or without NAC treatment. We observed activation of p38MAPK in $TERT^{-/-}$, $ATM^{-/-}$, and $ATM^{-/-}TERT^{-/-}$ LSKs, and this p38MAPK activation was completely abolished after in vivo treatment with NAC (Figure 6E). Further, treatment of LSKs with the p38MAPK inhibitor SB203580 blocked apoptosis induced by ROS, although it was a partial effect in $TERT^{-/-}$ and $ATM^{-/-}TERT^{-/-}$ LSKs (Figure 6F). This indicated that the p38MAPK pathway forms a part of the TERT-based protective mechanism for HSCs. However, JNK inhibitor SP600125 failed to rescue ROS-induced apoptosis in any of the HSCs. These results suggested that activation of p38MAPK causes ROS-induced apoptosis in $TERT^{-/-}$ HSCs, as well as in $ATM^{-/-}$ HSCs.

The fact that treatment with a p38MAPK inhibitor could not completely rescue ROS-induced apoptosis in TERT-deficient HSCs suggests that mechanisms other than p38MAPK exist through which TERT protect HSCs from ROS stress. The most well-known candidate for this is p53-mediated apoptosis.[44] This may in turn be mediated by B-cell lymphoma-2 (BCL-2) family proteins, such as PUMA or BAX, while these proteins can also regulate p53-independent apoptosis. Hence, we measured the activation of these molecules in WT, $TERT^{-/-}$, $ATM^{-/-}$, and $ATM^{-/-}TERT^{-/-}$ LSKs. While there was no difference in the transcription of p53, BAX and BCL-XL among LSKs of all genotypes, the expression of PUMA was elevated in $ATM^{-/-}$ and $ATM^{-/-}TERT^{-/-}$ LSKs, and BCL-2 was decreased in $TERT^{-/-}$ and $ATM^{-/-}TERT^{-/-}$ LSKs (Figure 6G and data not shown). These data indicate that PUMA is dependent on $ATM^{-/-}$ for activation and BCL-2 expression is maintained by TERT, and that these are regulated p53-independent manner. Moreover, BCL-2 is suggested to be involved in the regulation of apoptosis by TERT in HSCs, and PUMA and BCL-2 are suggested to act synergistically to enhance apoptosis in $ATM^{-/-}TERT^{-/-}$ LSKs.

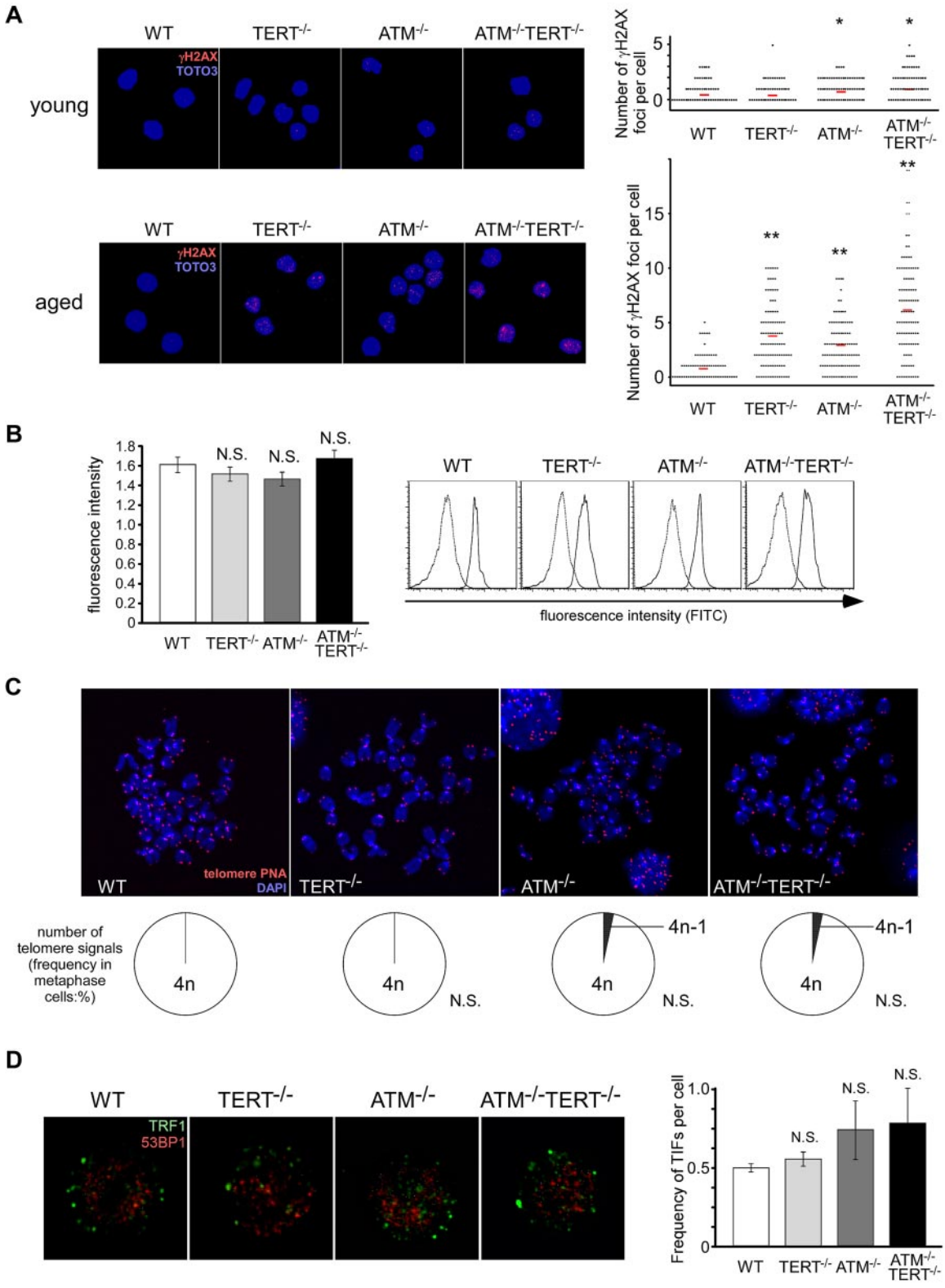

Figure 5. Alteration of telomeres is unlikely to be responsible for the impairment of the HSC pool seen in ATM and TERT doubly deficient mice. (A) Increased γH2AX foci in aged ATM$^{-/-}$ and TERT$^{-/-}$ LSKs, and significantly further increased γH2AX foci in aged ATM$^{-/-}$ TERT$^{-/-}$ LSKs (bottom). In young ATM$^{-/-}$ and ATM$^{-/-}$TERT$^{-/-}$ mice, γH2AX foci are only mildly increased (top). LSKs from mice of the indicated genotypes were stained with anti-γH2AX Ab (red), and TOTO3 staining was used to detect nuclei (blue; left: magnification ×600). The numbers of γH2AX foci in each cell were counted (right; *$P < .05$, **$P < .01$). (B) Relative telomere length of LSKs (left), measured by flow FISH. There are no apparent differences in telomere length among the different genotypes. Original FACS plots of flow FISH are shown (right). The 2 peaks in each plot are correspondent to signals in cells labeled with the telomere PNA probe and in unlabeled cells as a control. (C) Telomere FISH analysis of cells in metaphase. Representative pictures (top: magnification ×5000) and frequencies of telomere signals per cell (bottom) are shown. No alteration of telomere signals was detected in cells from mice of any of the genotypes. (D) No significant increase of TIFs in LSKs of all genotypes. LSKs from the indicated genotypes were costained with anti-TRF1 Ab (green) and anti-53BP1 Ab (red), nuclei were detected using DAPI staining (blue: left: magnification ×7000). The mean frequency (± SD) of merged yellow signals in each cell was determined by counting (right; *$P < .05$).

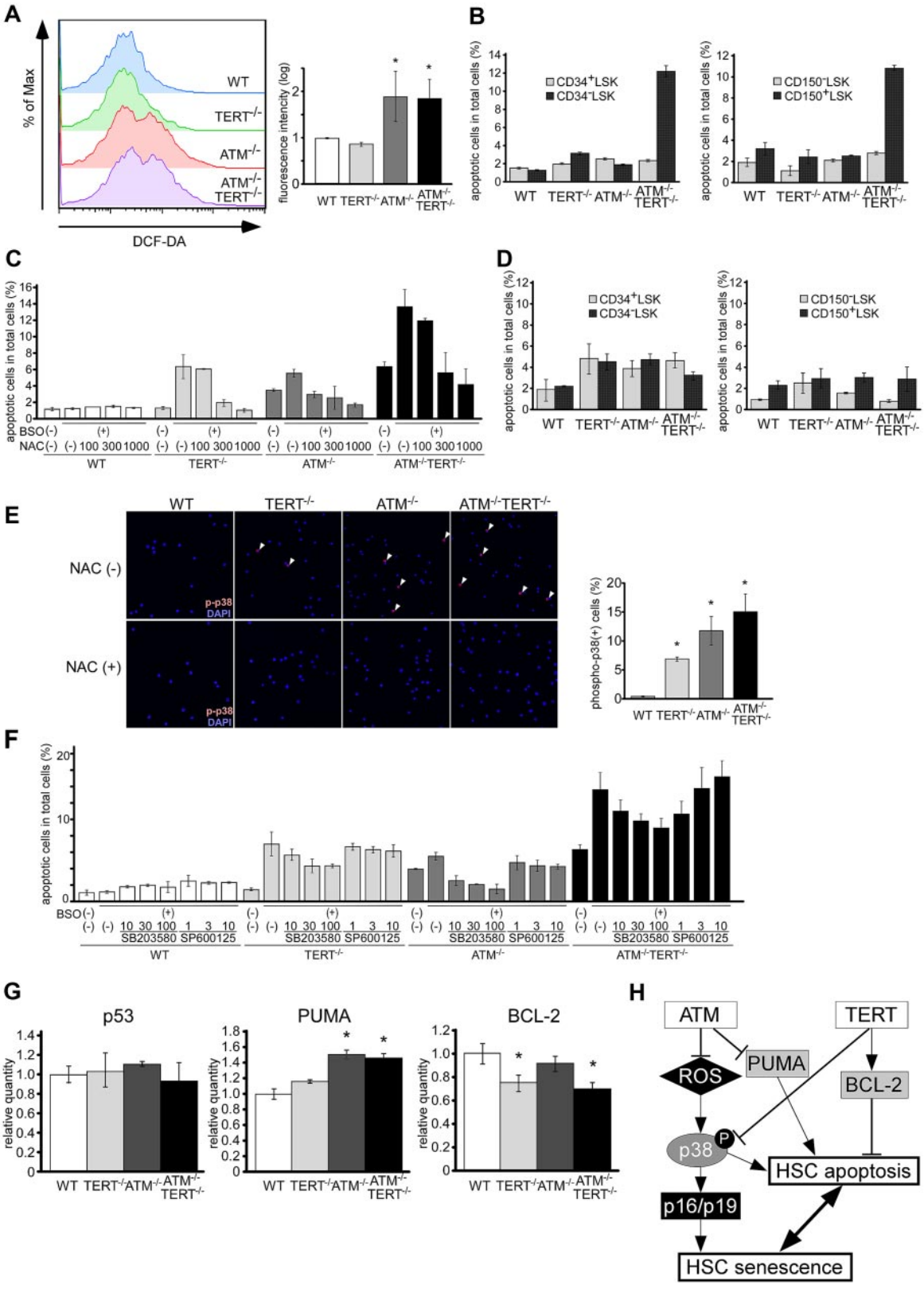

Figure 6. Apoptosis is induced in ATM and TERT doubly deficient HSCs as a result of ROS fragility and is regulated by p38MAPK and BCL-2 family proteins. (A) ROS levels in LSKs of the indicated genotypes. Comparable ROS levels in WT and TERT$^{-/-}$ LSKs, compared with elevated ROS in ATM$^{-/-}$ and ATM$^{-/-}$TERT$^{-/-}$ LSKs, were observed. Representative FACS analysis profiles derived from 3 experiments (left) and fluorescence intensity relative to WT (mean ± SD; right) are shown (*$P < .05$, n = 3). (B) Native apoptosis of CD34^{+}/CD34^{-} LSKs or CD150^{-}/CD150^{+} LSKs. Freshly isolated CD34^{+}/CD34^{-} LSKs or CD150^{-}/CD150^{+} LSKs from mice of each genotype were stained with annexin V and PI. CD34^{-} LSKs and CD150^{+} LSKs in ATM$^{-/-}$TERT$^{-/-}$ mice showed significantly higher apoptosis rates compared with the other genotypes. Data shown represent the mean percentage (± SD) of annexin V–positive cells out of total analyzed cells (n = 3). (C) Apoptosis following ROS induction. LSKs from WT, TERT$^{-/-}$, ATM$^{-/-}$, or ATM$^{-/-}$TERT$^{-/-}$ mice were cultured with or without BSO and/or NAC. After 12 hours of culture, harvested cells were stained with annexin V and PI. Apoptosis was induced in TERT$^{-/-}$, ATM$^{-/-}$, and ATM$^{-/-}$TERT$^{-/-}$ LSKs by BSO, and was rescued by adding NAC in a dose-dependent manner in all groups. Note: apoptosis was already

Discussion

Growing evidence suggests that TERT has major functions contributing to the prevention of aging by maintaining stem cell activity, and that these functions are unrelated to telomere lengthening.[12] However, it has been difficult to clarify the role of TERT in individual aging because of the length of time required for knockdown effects to become apparent and for oncogenesis to take place in response to overexpression. In this study, by examining the function of TERT in ATM-deficient mice, we have now successfully revealed that TERT plays a critical telomere-independent role in in vivo organismal aging.

Pathophysiologic aging of tissues is caused by decreasing stem cell activity, especially in tissues with high turnover, such as blood, gut, and skin. Perhaps as a mechanism to counter this, telomerase activity is primarily restricted to primitive stem and progenitor cell compartments.[45] Corresponding to this aging dogma, here we have demonstrated important roles for TERT in maintaining the stem cell activities in the hematopoietic system in an ATM-null background. We demonstrated in the current study that TERT-mediated aging in hematopoietic systems is regulated by $p16^{INK4a}$ and $p19^{ARF}$, but not by p21. We previously found that ATM is also regulated by these same proteins.[15] Cellular senescence triggered by telomere shortening is mediated through a pathway involving ATM, p53, and p21, but not $p16^{INK4a}$.[38,39] Therefore, these results also indicated that aging in ATM- or TERT-null HSCs is mediated through mechanisms other than telomere alteration. In support of this, telomere FISH and TIFs analysis also revealed that no telomere shortening or telomere dysfunction is mediated by the loss of TERT or the combination of ATM and TERT.

Aging is associated with a rise in intracellular ROS levels.[46,47] Increased ROS within HSCs caused by ATM deficiency results in the activation of the p38MAPK pathway.[16] Here, we clarified that TERT-deficient HSCs are vulnerable to the threat of apoptosis via ROS stress; hence, it was clearly indicated that TERT can protect HSCs from apoptosis induced by ROS stress. Various mechanisms of apoptosis induction in response to ROS stress are known. Current study showed that p38MAPK activation is also involved in ROS-induced apoptosis in TERT-deficient HSCs.

Although it is clear that TERT can partially protect HSCs from ROS-induced apoptosis via p38MAPK activation, our results suggest other mechanisms through which TERT regulates apoptosis in HSCs. BCL-2 family proteins, which include PUMA, BAX, and BCL-2, are reported to mediate apoptosis in HSCs.[48,49] While PUMA is known to enhance apoptosis in response to DNA damage, BCL-2 regulates apoptosis negatively. These proteins are reported to respond to ROS by regulating the release of cytochrome C from mitochondria, which in turn leads to apoptosis.[50] Here we showed that ATM deficiency activates PUMA and that TERT deficiency diminishes the expression of BCL-2. Loss of ATM may cause DNA damage in HSCs, and this may in turn activate PUMA. Maintenance of BCL-2 expression is suggested to be another mechanism besides p38MAPK-based regulation through which TERT protects HSCs from ROS stress (Figure 6H).

The present study has shown that the aging-related regulation of stem cells is mediated by apoptosis under ROS stress, and that TERT provides protection against this response. As ATM is responsive not only to ROS but also to DNA damage and a variety of other stresses, the telomere-independent, protective roles of TERT against extrinsic aging-related stresses may also include responses not only to ROS but also to a variety of other stresses, such as extracellular damaging agents or mitochondria-dependent cell death. Thus, both ATM and TERT contribute to the mitigation of aging by maintaining stem cells, albeit through separate mechanisms. These findings will prove to be valuable assets for understanding the regulation of hematopoietic stem cells, especially under conditions of stress.

Acknowledgments

We thank Dr Ryo Funayama (Tohoku University, Sendai, Japan) for helpful discussion, Ayako Kumakubo and Naoko Tago for technical assistance, and Hiroko Iwasaki for help in manuscript preparation.

This work was supported by a Grant-in-Aid for Scientific Research on Innovative Areas "Cancer Stem Cells" from the Ministry of Education, Culture, Sports, Science, and Technology (MEXT) of Japan, the Global COE program "Education and Research Center for Stem Cell Medicine" of Keio University, and a Grant-in-Aid for Japan Society for the Promotion of Science Fellows. E.N. is a Research Fellow of the Japan Society for the Promotion of Science.

Authorship

Contribution: E.N. designed the research, performed the experiments, analyzed and interpreted the data, and wrote the manuscript; M.Y. performed the experiments; K.H. and K.T. assisted in experiment design; M.X. maintained mice; F.A. and S.N. assisted in research design and in manuscript preparation; and T.S. directed the project, secured funding and assisted in manuscript preparation.

Conflict-of-interest disclosure: The authors declare no competing financial interests.

Correspondence: Toshio Suda, MD, PhD, 35 Shinano-machi, Shinjuku-ku, Tokyo 160-8582, Japan; e-mail: sudato@sc.itc.keio.ac.jp.

Figure 6. (continued) induced in $ATM^{-/-}TERT^{-/-}$ LSKs in culture without BSO to some extent. The data shown represent the mean percentage (± SD) of annexin V–positive cells (n = 4). (D) Native apoptosis of $CD34^+/CD34^-$ LSKs or $CD150^-/CD150^+$ LSKs in NAC-administered mice. Freshly isolated $CD34^+/CD34^-$ LSKs or $CD150^-/CD150^+$ LSKs from mice treated with NAC were stained with annexin V and PI as for panel B. Native apoptosis of $CD34^-$ LSKs or $CD150^+$ LSKs seen in $ATM^{-/-}TERT^{-/-}$ mice is completely rescued. (E) Activation of p38MAPK in $TERT^{-/-}$, $ATM^{-/-}$, or $ATM^{-/-}TERT^{-/-}$ murine LSKs (top), which is completely rescued in LSKs from NAC-treated mice in vivo (bottom). LSKs from the indicated genotypes were stained with anti–phospho-p38MAPK Ab (red) and DAPI for nuclear stain (blue: magnification ×400). Representative pictures (left) and the mean ratios (± SD) of phosphorylated p38MAPK-positive cells in untreated LSKs (right) are shown. (F) Rescued ROS-induced apoptosis in LSKs by a p38MAPK inhibitor. LSKs from WT, $TERT^{-/-}$, $ATM^{-/-}$, or $ATM^{-/-}TERT^{-/-}$ mice were treated with BSO, and then, for rescue, with a p38MAPK inhibitor, SB203580, or a JNK inhibitor, SP600125. Annexin V staining assays were performed as for panel C. While apoptosis induced in $ATM^{-/-}$ LSKs by BSO was completely rescued by adding SB203580, in a dose-dependent manner, rescue was only partial in $TERT^{-/-}$ and $ATM^{-/-}TERT^{-/-}$ LSKs. The addition of SP600125, on the other hand, did not result in rescue. (G) Expression of apoptosis-related genes in aged murine HSCs. qPCR analysis of p53, PUMA, and BCL-2 in LSKs from mice of the indicated genotypes. While p53 expression was comparable among all groups, elevated PUMA expression in $ATM^{-/-}$ and $ATM^{-/-}TERT^{-/-}$ LSKs and decreased BCL-2 expression in $TERT^{-/-}$ and $ATM^{-/-}TERT^{-/-}$ LSKs were seen. Data shown are the mean ratio (± SD) of mRNA to β-actin levels (*$P < .05$, n = 4). (H) Schematic summarizing the role of ATM and TERT in HSCs.

References

1. Rando TA. Stem cells, ageing and the quest for immortality. *Nature.* 2006;441(7097):1080-1086.
2. Ahmed S, Passos JF, Birket MJ, et al. Telomerase does not counteract telomere shortening but protects mitochondrial function under oxidative stress. *J Cell Sci.* 2008;121(Pt 7):1046-1053.
3. Chung HK, Cheong C, Song J, Lee HW. Extratelomeric functions of telomerase. *Curr Mol Med.* 2005;5(2):233-241.
4. Parkinson EK, Fitchett C, Cereser B. Dissecting the non-canonical functions of telomerase. *Cytogenet Genome Res.* 2008;122(3-4):273-280.
5. Kipling D, Cooke HJ. Hypervariable ultra-long telomeres in mice. *Nature.* 1990;347(6291):400-402.
6. Allsopp RC, Morin GB, DePinho R, Harley CB, Weissman IL. Telomerase is required to slow telomere shortening and extend replicative lifespan of HSCs during serial transplantation. *Blood.* 2003;102(2):517-520.
7. Allsopp RC, Morin GB, Horner JW, DePinho R, Harley CB, Weissman IL. Effect of TERT overexpression on the long-term transplantation capacity of hematopoietic stem cells. *Nat Med.* 2003;9(4):369-371.
8. Flores I, Cayuela ML, Blasco MA. Effects of telomerase and telomere length on epidermal stem cell behavior. *Science.* 2005;309(5738):1253-1256.
9. Sarin KY, Cheung P, Gilison D, et al. Conditional telomerase induction causes proliferation of hair follicle stem cells. *Nature.* 2005;436(7053):1048-1052.
10. Choi J, Southworth LK, Sarin KY, et al. TERT promotes epithelial proliferation through transcriptional control of a Myc- and Wnt-related developmental program. *PLoS Genet.* 2008;4(1):e10.
11. Geserick C, Blasco MA. Novel roles for telomerase in aging. *Mech Ageing Dev.* 2006;127(6):579-583.
12. Tomas-Loba A, Flores I, Fernandez-Marcos PJ, et al. Telomerase reverse transcriptase delays aging in cancer-resistant mice. *Cell.* 2008;135(4):609-622.
13. Shiloh Y. ATM and related protein kinases: safeguarding genome integrity. *Nat Rev Cancer.* 2003;3(3):155-168.
14. Guo Z, Kozlov S, Lavin MF, Person MD, Paull TT. ATM activation by oxidative stress. *Science.* 2010;330(6003):517-521.
15. Ito K, Hirao A, Arai F, et al. Regulation of oxidative stress by ATM is required for self-renewal of haematopoietic stem cells. *Nature.* 2004;431(7011):997-1002.
16. Ito K, Hirao A, Arai F, et al. Reactive oxygen species act through p38 MAPK to limit the lifespan of hematopoietic stem cells. *Nat Med.* 2006;12(4):446-451.
17. Lavin MF. Ataxia-telangiectasia: from a rare disorder to a paradigm for cell signalling and cancer. *Nat Rev Mol Cell Biol.* 2008;9(10):759-769.
18. Xu Y. DNA damage: a trigger of innate immunity but a requirement for adaptive immune homeostasis. *Nat Rev Immunol.* 2006;6(4):261-270.
19. Herzog KH, Chong MJ, Kapsetaki M, Morgan JI, McKinnon PJ. Requirement for Atm in ionizing radiation-induced cell death in the developing central nervous system. *Science.* 1998;280(5366):1089-1091.
20. Yuan X, Ishibashi S, Hatakeyama S, et al. Presence of telomeric G-strand tails in the telomerase catalytic subunit TERT knockout mice. *Genes Cells.* 1999;4(10):563-572.
21. Yamazaki S, Iwama A, Takayanagi S, et al. Cytokine signals modulated via lipid rafts mimic niche signals and induce hibernation in hematopoietic stem cells. *EMBO J.* 2006;25(15):3515-3523.
22. van Pelt K, de Haan G, Vellenga E, Daenen SM. Administration of low-dose cytarabine results in immediate S-phase arrest and subsequent activation of cell cycling in murine stem cells. *Exp Hematol.* 2005;33(2):226-231.
23. Liu Y, Snow BE, Hande MP, et al. The telomerase reverse transcriptase is limiting and necessary for telomerase function in vivo. *Curr Biol.* 2000;10(22):1459-1462.
24. Morrison SJ, Wandycz AM, Akashi K, Globerson A, Weissman IL. The aging of hematopoietic stem cells. *Nat Med.* 1996;2(9):1011-1016.
25. Rossi DJ, Bryder D, Zahn JM, et al. Cell intrinsic alterations underlie hematopoietic stem cell aging. *Proc Natl Acad Sci U S A.* 2005;102(26):9194-9199.
26. Sudo K, Ema H, Morita Y, Nakauchi H. Age-associated characteristics of murine hematopoietic stem cells. *J Exp Med.* 2000;192(9):1273-1280.
27. Beerman I, Maloney WJ, Weissmann IL, Rossi DJ. Stem cells and the aging hematopoietic system. *Curr Opin Immunol.* 2010;22(4):500-506.
28. Ito K, Takubo K, Arai F, et al. Regulation of reactive oxygen species by Atm is essential for proper response to DNA double-strand breaks in lymphocytes. *J Immunol.* 2007;178(1):103-110.
29. Miller JP, Allman D. The decline in B lymphopoiesis in aged mice reflects loss of very early B-lineage precursors. *J Immunol.* 2003;171(5):2326-2330.
30. Kim M, Moon HB, Spangrude GJ. Major age-related changes of mouse hematopoietic stem/progenitor cells. *Ann N Y Acad Sci.* 2003;996:195-208.
31. Liang Y, Van Zant G, Szilvassy SJ. Effects of aging on the homing and engraftment of murine hematopoietic stem and progenitor cells. *Blood.* 2005;106(4):1479-1487.
32. Narita M, Nunez S, Heard E, et al. Rb-mediated heterochromatin formation and silencing of E2F target genes during cellular senescence. *Cell.* 2003;113(6):703-716.
33. Zhang R, Poustovoitov MV, Ye X, et al. Formation of MacroH2A-containing senescence-associated heterochromatin foci and senescence driven by ASF1a and HIRA. *Dev Cell.* 2005;8(1):19-30.
34. Rossi DJ, Bryder D, Seita J, Nussenzweig A, Hoeijmakers J, Weissman IL. Deficiencies in DNA damage repair limit the function of haematopoietic stem cells with age. *Nature.* 2007;447(7145):725-729.
35. Rossi DJ, Jamieson CH, Weissman IL. Stems cells and the pathways to aging and cancer. *Cell.* 2008;132(4):681-696.
36. Wang C, Jurk D, Maddick M, Nelson G, Martin-Ruiz C, von Zglinicki T. DNA damage response and cellular senescence in tissues of aging mice. *Aging Cell.* 2009;8(3):311-323.
37. Sokolov MV, Dickey JS, Bonner WM, Sedelnikova OA. gamma-H2AX in bystander cells: not just a radiation-triggered event, a cellular response to stress mediated by intercellular communication. *Cell Cycle.* 2007;6(18):2210-2212.
38. Herbig U, Jobling WA, Chen BP, Chen DJ, Sedivy JM. Telomere shortening triggers senescence of human cells through a pathway involving ATM, p53, and p21(CIP1), but not p16(INK4a). *Mol Cell.* 2004;14(4):501-513.
39. Takai H, Smogorzewska A, de Lange T. DNA damage foci at dysfunctional telomeres. *Curr Biol.* 2003;13(17):1549-1556.
40. Opferman JT, Iwasaki H, Ong CC, et al. Obligate role of anti-apoptotic MCL-1 in the survival of hematopoietic stem cells. *Science.* 2005;307(5712):1101-1104.
41. Wilson A, Murphy MJ, Oskarsson T, et al. c-Myc controls the balance between hematopoietic stem cell self-renewal and differentiation. *Genes Dev.* 2004;18(22):2747-2763.
42. Cao Y, Li H, Deb S, Liu JP. TERT regulates cell survival independent of telomerase enzymatic activity. *Oncogene.* 2002;21(20):3130-3138.
43. Rahman R, Latonen L, Wiman KG. hTERT antagonizes p53-induced apoptosis independently of telomerase activity. *Oncogene.* 2005;24(8):1320-1327.
44. Liu Y, Elf SE, Asai T, et al. The p53 tumor suppressor protein is a critical regulator of hematopoietic stem cell behavior. *Cell Cycle.* 2009;8(19):3120-3124.
45. Harrington L. Does the reservoir for self-renewal stem from the ends? *Oncogene.* 2004;23(43):7283-7289.
46. Haendeler J, Hoffmann J, Brandes RP, Zeiher AM, Dimmeler S. Hydrogen peroxide triggers nuclear export of telomerase reverse transcriptase via Src kinase family-dependent phosphorylation of tyrosine 707. *Mol Cell Biol.* 2003;23(13):4598-4610.
47. Haendeler J, Hoffmann J, Diehl JF, et al. Antioxidants inhibit nuclear export of telomerase reverse transcriptase and delay replicative senescence of endothelial cells. *Circ Res.* 2004;94(6):768-775.
48. Yu H, Shen H, Yuan Y, et al. Deletion of Puma protects hematopoietic stem cells and confers long-term survival in response to high-dose gamma-irradiation. *Blood.* 2010;115(17):3472-3480.
49. Domen J, Cheshier SH, Weissman IL. The role of apoptosis in the regulation of hematopoietic stem cells: Overexpression of Bcl-2 increases both their number and repopulation potential. *J Exp Med.* 2000;191(2):253-264.
50. Taylor RC, Cullen SP, Martin SJ. Apoptosis: controlled demolition at the cellular level. *Nat Rev Mol Cell Biol.* 2008;9(3):231-241.